Effects of P doping on photoluminescence of $Si_{1-x}Ge_x$ alloy nanocrystals embedded in SiO_2 matrices: Improvement and degradation of luminescence efficiency

Kimiaki Toshikiyo, Masakazu Tokunaga, and Shinji Takeoka
Graduate School of Science and Technology, Kobe University, Rokkodai, Nada, Kobe 657-8501, Japan

Minoru Fujii[a] and Shinji Hayashi
Department of Electrical and Electronics Engineering, Faculty of Engineering, Kobe University, Rokkodai, Nada, Kobe 657-8501, Japan

Kazuyuki Moriwaki
Graduate School of Science and Technology, Kobe University, Rokkodai, Nada, Kobe 657-8501, Japan

(Received 14 May 2001; accepted for publication 28 August 2001)

The effects of P doping on photoluminescence (PL) properties of $Si_{1-x}Ge_x$ alloy nanocrystals (nc-$Si_{1-x}Ge_x$) in SiO_2 thin films were studied. P doping drastically decreases the electron spin resonance (ESR) signals that are assigned to the Si and Ge dangling bonds at the interfaces between nc-$Si_{1-x}Ge_x$ and SiO_2 matrices (Si and Ge P_b centers). With increasing P concentration, the signal from the Ge P_b centers are first quenched, and then the signal from the Si P_b centers start to be quenched. The quenching of the ESR signals is accompanied by a drastic enhancement of the PL intensity. The PL intensity has a maximum at a certain P concentration, which depends on the Si:Ge ratio. By further increasing the P concentration, the PL intensity becomes weaker. In this P concentration range, optical absorption emerges due to the intravalley transition of free electrons generated by the P doping. The observation of the free-electron absorption provides direct evidence that carriers in nanometer-sized $Si_{1-x}Ge_x$ alloy crystals can be controlled by impurity doping. © *2001 American Institute of Physics.* [DOI: 10.1063/1.1413486]

I. INTRODUCTION

During the past decade, nanometer-sized Si crystals (nc-Si) have been intensively investigated because they are believed to be promising materials for novel optical or electro-optical devices and offer a good model system to study zero-dimensional quantum size effects in indirect-gap semiconductors. A continuous shift of the photoluminescence (PL) energy from the bulk band gap to the visible region has been observed with a decrease of the nanocrystal size.[1–6] The observed strong size dependence indicates that the PL is due to the recombination of excitons confined in zero-dimensional Si quantum dots.

The quantum confinement effect enhances the possibility of no-phonon (NP) quasi-direct optical transitions. However, the indirect band-gap nature of bulk Si crystal is still preserved even for nc-Si several nanometers in diameter.[7] This results in a relatively long PL lifetime, which is one of the obstacles in achieving Si-based light-emitting devices. Therefore a new approach to shorten the radiative exciton lifetime further is highly desired.

NP transitions can be enhanced by $Si_{1-x}Ge_x$ alloy formation. In a bulk $Si_{1-x}Ge_x$ alloy, the enhancement of the NP transition oscillator strength can be observed due to the breakdown of the *k*-conservation rule arising from the violation of the translational symmetry of the crystalline lattice.[8] Similar effects have been successfully observed in nanometer-sized $Si_{1-x}Ge_x$ alloy crystals (nc-$Si_{1-x}Ge_x$).[9–11] In resonant PL spectra of nc-$Si_{1-x}Ge_x$, structures corresponding to momentum conserving phonons are smeared out by increasing the Ge concentration.[9] Furthermore, the radiative lifetime is shortened with this increasing Ge concentration.[9–12] These results provide strong evidence that the oscillator strength of nc-Si is enhanced by $Si_{1-x}Ge_x$ alloy formation.

However, in actual nc-$Si_{1-x}Ge_x$, the luminescence efficiency is smaller than that of pure nc-Si.[12] In a previous work we prepared nc-$Si_{1-x}Ge_x$ as small as 4 nm in diameter embedded in SiO_2 thin films with different Ge concentrations and studied the electron spin resonance (ESR) and PL properties.[13] The ESR data indicated that Ge dangling bonds are generated at the interfaces between nc-$Si_{1-x}Ge_x$ and SiO_2 matrices (Ge P_b centers), and that the number of Ge P_b centers increases with the Ge concentration. From a comparison between these two measurements, we could conclude that Ge P_b centers act as efficient nonradiative recombination centers for photogenerated carriers, resulting in the quenching of the PL. In order to make good use of the advantages of nc-$Si_{1-x}Ge_x$ mentioned above, the elimination of surface defects is indispensable.

For pure nc-Si in SiO_2 matrices, the passivation of Si dangling-bond defects (Si P_b centers) by hydrogen and oxygen has been reported to be effective in improving the luminescence efficiency.[14,15] Recently, we demonstrated that Si P_b centers can be effectively passivated by P doping, leading

[a]Author to whom correspondence should be addressed. Electronic mail: fujii@eedept.kobe-u.ac.jp

to the significant enhancement of the PL efficiency.[16–18] For nc-$Si_{1-x}Ge_x$, the passivation of Ge P_b centers in a similar way might be possible.

In this work we prepared P-doped nc-$Si_{1-x}Ge_x$ as small as 4 nm in diameter with different P concentrations embedded in phosphosilicate glass (PSG) thin films and studied the ESR and PL properties. It will be shown that the density of not only Si but also Ge P_b centers decreases with increasing P concentration. The decrease in the defect density results in a dramatic improvement of the PL efficiency. However, by further increasing the P concentration, the PL intensity decreases. The quenching of the PL is accompanied by the appearance of optical absorption in the infrared range. The mechanism causing this improvement and degradation of the PL efficiency by P doping will be discussed.

II. EXPERIMENT

P doped $Si_{1-x}Ge_x$ alloy nanocrystals were prepared by the same method as used in our previous work.[9,12] The Si, Ge, SiO_2, and PSG sputtering targets were simultaneously sputtered in Ar gas of 0.3 Pa using a multitarget sputtering apparatus. The substrates were fused quartz plates. The thickness of the films for PL measurements was about 700 nm, and that for ESR and optical absorption measurements about 8.4 μm. The Ge and P concentrations (mol %) in the films were controlled by changing the sputtering power and the distance between the substrate and the target for the four sputtering guns independently. After the deposition, the films were annealed in an N_2 gas atmosphere for 30 min at 1100 °C. During the annealing nc-$Si_{1-x}Ge_x$ were grown in PSG matrices. The P and Ge concentrations were determined by electron probe microanalysis and Raman spectroscopy,[12,19] respectively. The P concentration varied from 0 (without P doping) to about 1.0 mol %. The Ge concentration (x) varied from 0.1 to 0.3. The size of nc-$Si_{1-x}Ge_x$ was estimated from cross-sectional high-resolution transmission electron microscopic (HRTEM) images. These HRTEM observations revealed that spherical nanocrystals as small as 4 to 5 nm in diameter grow in amorphous PSG matrices. Each nanocrystal was found to be isolated from the others by PSG barriers several nanometers in thickness. The PL spectra were measured using a single monochromator equipped with a liquid N_2 cooled Ge detector. The excitation source was the 488.0 nm line of an Ar ion laser. The spectra were measured in the temperature range between 10 and 300 K in a continuous-flow He cryostat. The X-band ESR was measured by using a conventional ESR spectrometer at room temperature. The intensity of the ESR signals was calibrated by simultaneously measuring the signals from a fixed amount of Mn^{2+}/MgO powder. The optical absorption spectra were measured in the range between 0.19 and 3.2 μm. To obtain the absorption coefficients of nc-$Si_{1-x}Ge_x$ the measured absorption spectra (absorbance) were divided by the film thickness and the volume fraction of nc-$Si_{1-x}Ge_x$.

III. RESULTS

Figure 1(a) shows PL spectra of nc-$Si_{0.9}Ge_{0.1}$ for various P concentrations at 10 K. PL peaks can be observed at around 1.44 and 0.9 eV. The 1.44 eV peak corresponds to the band-edge PL. The 0.9 eV peak can only be observed at low temperatures and is generally assigned to the recombination of photoexcited carriers via Si P_b centers.[16,17,20,21] Figure 1(b) shows PL spectra of nc-$Si_{0.7}Ge_{0.3}$ at 10 K. A band-edge PL peak can be observed at around 1.40 eV. The integrated intensities of the band-edge PL and the 0.9 eV PL are shown in Fig. 2 as a function of the P concentration. The vertical axis represents the intensity with respect to the band-edge PL intensity of nc-$Si_{0.9}Ge_{0.1}$ in SiO_2 (without P doping). First of all, it should be noted that the intensity of the band-edge PL

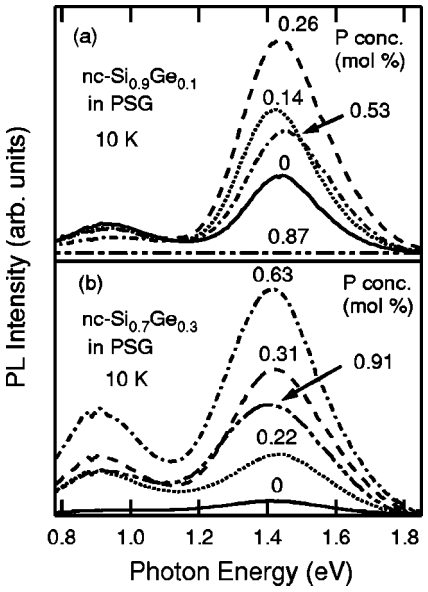

FIG. 1. Photoluminescence from nc-$Si_{1-x}Ge_x$ with (a) $x=0.1$ and (b) $x=0.3$ dispersed in PSG thin films at 10 K.

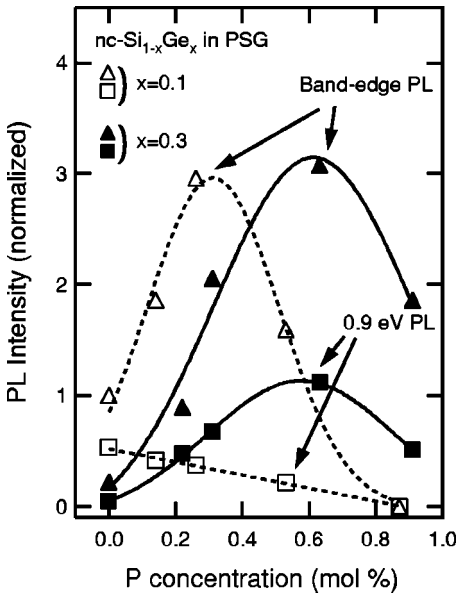

FIG. 2. Intensities of the band-edge PL (△ and ▲) and Si-P_b-center-related PL (□ and ■) at 10 K as a function of P concentration. Open symbols are for nc-$Si_{0.9}Ge_{0.1}$ and closed symbols are for nc-$Si_{0.7}Ge_{0.3}$. The vertical axis represents the PL intensity with respect to the band-edge PL intensity of nc-$Si_{0.9}Ge_{0.1}$ in SiO_2.

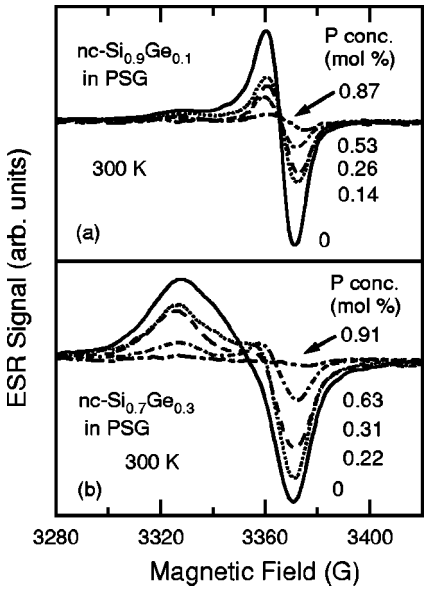

FIG. 3. ESR derivative spectra of nc-$Si_{1-x}Ge_x$ dispersed in PSG thin films at room temperature.

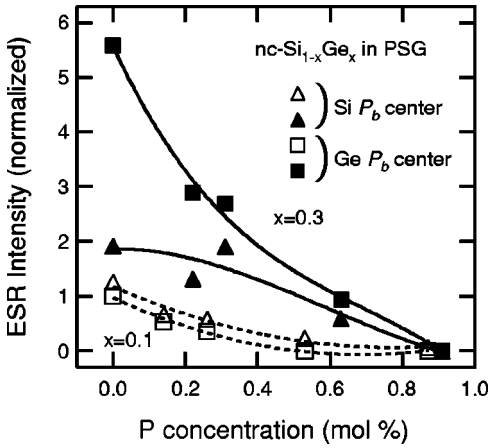

FIG. 4. Integrated intensities of ESR signals from Si (△ and ▲) and Ge (□ and ■) P_b centers as a function of P concentration. Open symbols are for nc-$Si_{0.9}Ge_{0.1}$ and closed symbols are for nc-$Si_{0.7}Ge_{0.3}$. The vertical axis represents the ESR intensity with respect to the intensity of Ge P_b centers in nc-$Si_{0.9}Ge_{0.1}$ in SiO_2.

for nc-$Si_{0.7}Ge_{0.3}$ in SiO_2 is much smaller than that for nc-$Si_{0.9}Ge_{0.1}$. This Ge concentration dependence of the PL intensity is generally observed for nc-$Si_{1-x}Ge_x$ in pure SiO_2.[13] With increasing P concentration, the intensities of the band-edge PL for both samples first increase and then decrease. This behavior can be observed over the entire temperature range (10–300 K). The maximum PL intensities are almost the same for both series of samples and are also almost the same as the maximum PL intensity measured on P doped pure nc-Si.[16,17] Since the PL intensity of nc-$Si_{0.7}Ge_{0.3}$ in pure SiO_2 is smaller than that of nc-$Si_{0.9}Ge_{0.1}$, the degree of improvement in the band-edge PL efficiency is higher for nc-$Si_{0.7}Ge_{0.3}$; the PL intensity of nc-$Si_{0.9}Ge_{0.1}$ is improved by a factor of 3 while that of nc-$Si_{0.7}Ge_{0.3}$ by a factor of 14. In Fig. 2, in contrast to the band-edge PL, the P concentration dependence of the 0.9 eV PL intensity is qualitatively different between the two samples. For nc-$Si_{0.9}Ge_{0.1}$, the intensity of the 0.9 eV PL decreases monotonously, while for nc-$Si_{0.7}Ge_{0.3}$ it has a maximum at 0.6 mol %.

Figures 3(a) and 3(b) show ESR derivative spectra of nc-$Si_{0.9}Ge_{0.1}$ and nc-$Si_{0.7}Ge_{0.3}$ doped for various P concentrations, respectively. For the samples without P doping, asymmetric ESR signals can be observed; the g value and the peak-to-peak linewidth are 2.0058 and 10.7 G for nc-$Si_{0.9}Ge_{0.1}$, and 2.0103 and 36.6 G for nc-$Si_{0.7}Ge_{0.3}$, respectively. These signals can be assigned to a superposition of signals from Si and Ge P_b centers.[13] As the P concentration increases, the intensity of the ESR signals decreases, while the g values and the peak-to-peak linewidths are almost constant over the entire P concentration range. Figure 4 shows integrated intensities of ESR signals for Si and Ge P_b centers as a function of the P concentration. The intensities are obtained by deconvoluting an ESR spectrum into two Lorentzian functions. The vertical axis represents the ESR intensity with respect to the intensity of the Ge P_b centers in nc-$Si_{0.9}Ge_{0.1}$ in pure SiO_2. It is worth noting that the ESR intensities of nc-$Si_{0.7}Ge_{0.3}$ in pure SiO_2 (in particular the intensity of the Ge P_b centers) are much larger than those of nc-$Si_{0.9}Ge_{0.1}$ in pure SiO_2. In nc-$Si_{0.9}Ge_{0.1}$, the intensities of the Si and Ge P_b centers decrease at almost the same rate with increasing P concentration, indicating that the number of Si and Ge P_b centers decreases monotonously with the P doping level. On the other hand, in nc-$Si_{0.7}Ge_{0.3}$, the Si and Ge P_b centers exhibit a different P concentration dependence; the intensity of the signal from the Ge P_b centers decreases rapidly with increasing P concentration, while that from the Si P_b centers remains almost constant within a low P concentration range and then decreases gradually with further increases in the P concentration.

Figure 5 shows optical absorption spectra for samples with different P concentrations. The periodic structures are

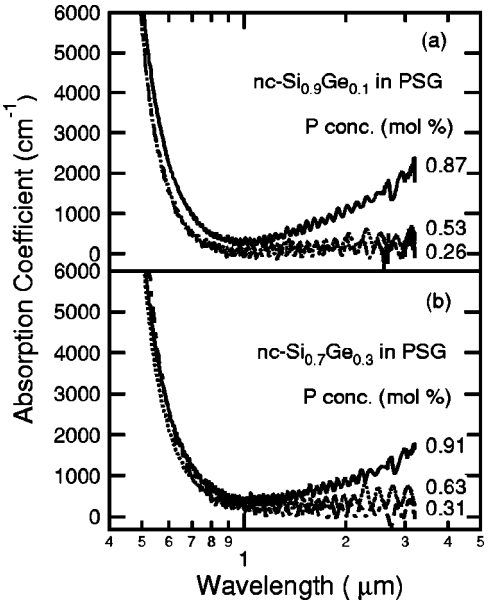

FIG. 5. Optical absorption spectra for nc-$Si_{1-x}Ge_x$ dispersed in PSG thin films at room temperature.

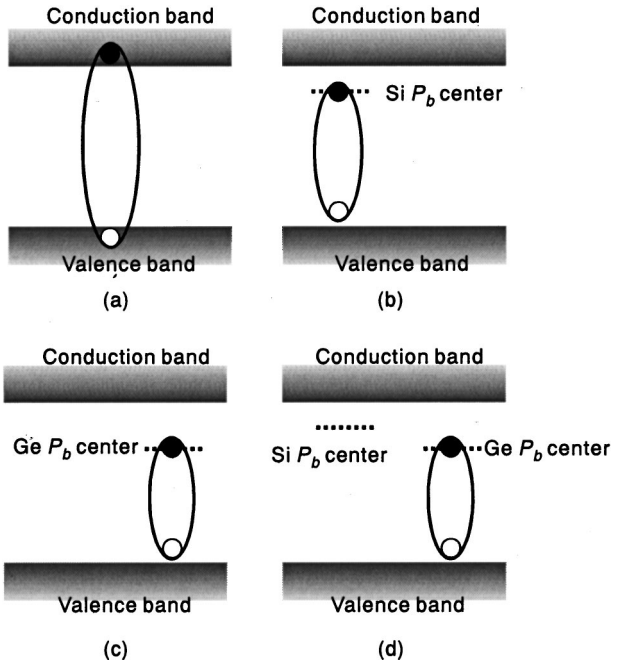

FIG. 6. Schematic band diagrams of nanocrystals (a) without defects, (b) with a Si P_b center, (c) with a Ge P_b center, and (d) with Si and Ge P_b centers.

due to the interference of the incidence light inside the films. For those samples with P concentrations smaller than 0.6 mol %, the absorption decreases monotonically towards the infrared region. This absorption is due to the valence-to-conduction-band transitions in nc-$Si_{1-x}Ge_x$ and/or transitions related to band tails or defects levels. On the other hand, for those samples with P concentrations larger than 0.6 mol %, a smoothly rising absorption continuum appears in the infrared region. A very similar absorption in the infrared range has been observed for P-doped nc-Si.[18] The infrared absorption is assigned to the intravalley transition of electrons generated by P doping in the conduction band, i.e., free-electron absorption in nc-Si. The free-electron absorption is characterized by a monotonic, structureless spectrum that grows as λ^p, where λ is the photon wavelength and the power p depends on the mode of scattering. The present infrared absorption can be well fitted with $\lambda^{1.5}$, suggesting that this absorption is accompanied by scattering by acoustic phonons.[22]

IV. DISCUSSION

The observed P concentration dependences of the PL and ESR properties as well as optical absorption spectra can consistently be explained by the following model. From the point of view of PL properties, nc-Si embedded in SiO_2 matrices (without Ge doping) can be classified into two categories. One is nc-Si without nonradiative recombination centers [Fig. 6(a)], which shows a slow band-edge PL at around 1.4 eV.[5] The other is nc-Si having at least one Si P_b center [Fig. 6(b)]. In these nanocrystals, photoexcited carriers are always trapped at the Si P_b centers and recombine via the centers. These nanocrystals do not show the band-edge PL but show only the 0.9 eV PL at low temperatures.

Through $Si_{1-x}Ge_x$ alloy formation, Ge P_b centers are introduced into both kinds of nanocrystals. As a result, nanocrystals with Ge P_b centers [Fig. 6(c)] and those with Si and Ge P_b centers [Fig. 6(d)] are formed. In these nanocrystals, photoexcited carriers are preferentially trapped at the Ge P_b centers and recombine nonradiatively even at low temperatures.[13] The present samples are ensembles of these four kinds of nanocrystals. With increasing Ge concentration, the number of nanocrystals with Ge P_b centers [Figs. 6(c) and 6(d)] increases, resulting in the quenching of both the band-edge PL and Si-P_b-center-related PL. In the present work we studied two series of samples with different Ge concentrations ($Si_{0.9}Ge_{0.1}$ and $Si_{0.7}Ge_{0.3}$). In the sample with the low Ge concentration, nanocrystals without defects [Fig. 6(a)] and with only Si P_b centers [Fig. 6(b)] were considered to be present to some extent. On the other hand, in the sample with the high Ge concentration, almost all of the nanocrystals were considered to have Ge P_b centers, resulting in an extremely weak band-edge PL and Si-P_b-center-related PL (see Fig. 2).

As can be clearly seen in Fig. 4, not only Si P_b centers but also Ge P_b centers are passivated by P doping. The passivation is considered to be made electrically, i.e., electrons supplied by the P doping become trapped at the P_b centers and disactivate them. In nc-$Si_{0.7}Ge_{0.3}$, the quenching of the ESR signal from a Ge P_b center is much faster than that from a Si P_b center. This result indicates that, if both Si and Ge P_b centers exist in one nc-$Si_{1-x}Ge_x$, electrons supplied by P doping are preferentially captured by the Ge P_b centers. After the passivation of the Ge P_b centers is completed, the passivation of the Si P_b centers starts.

This model can well explain the P concentration dependence of PL properties. Preferential passivation of Ge P_b centers increases the number of nanocrystals that do not have electrically active Ge P_b centers. As a result, in nc-$Si_{0.7}Ge_{0.3}$, the intensities of both the band-edge PL and Si-P_b-center-related PL increase by P doping, i.e., the Si P_b centers remain active even if the P concentration is relatively high. On the other hand, in nc-$Si_{0.9}Ge_{0.1}$, the number of nanocrystals having Ge P_b centers is small. Therefore the passivation of the Si P_b centers starts at a low P concentration, resulting in the quenching of the Si-P_b-center-related PL within the low P concentration region.

At a high P concentration, after the passivation of both the Si and Ge P_b centers is completed, electrically active P atoms supply free electrons in nc-$Si_{1-x}Ge_x$. The free-carrier absorption in Fig. 5 at a high P concentration gives direct evidence that free electrons are generated in nc-$Si_{1-x}Ge_x$. If such free electrons are supplied, three-body Auger recombination becomes possible among the electrons and photoexcited electron–hole pairs (eeh Auger process), i.e., the recombination energy of an electron–hole pair can be transferred to an electron with its following excitation to a higher energy in the conduction band. The lifetime of the eeh Auger recombination process in nc-Si is in the range of 0.1 and 1 ns.[23] This lifetime is several orders of magnitude shorter than the radiative lifetime of excitons in nc-$Si_{1-x}Ge_x$[9,12] and is also shorter than the Si-P_b-center-related PL.[24] Therefore the generation of free electrons results in a

significant decrease in the PL efficiency. The observed quenching of the PL intensity at a high P concentration can be explained by this model.

In Fig. 2 the value of the P concentration having the maximum PL intensity depends on the Ge concentration. The PL intensity of nc-$Si_{0.9}Ge_{0.1}$ has a maximum at 0.3 mol %, while that of nc-$Si_{0.7}Ge_{0.3}$ has one at 0.6 mol %. This indicates that a larger number of P atoms are required for nc-$Si_{0.7}Ge_{0.3}$ than for nc-$Si_{0.9}Ge_{0.1}$ to passivate Si and Ge P_b centers. This result is consistent with ESR data. As can be seen in Fig. 4, the total number of Si and Ge P_b centers for nc-$Si_{0.7}Ge_{0.3}$ in pure SiO_2 is much larger than that for nc-$Si_{0.9}Ge_{0.1}$ in pure SiO_2. Therefore to complete the passivation of all of the centers, a larger number of P atoms are necessary, resulting in a shift of the PL maximum to a high P concentration region.

V. CONCLUSION

The effects of P doping on the PL properties of nc-$Si_{1-x}Ge_x$ in SiO_2 thin films were studied. It was found that doped P atoms can play several different roles depending on the surface termination conditions. If P atoms are doped in nc-$Si_{1-x}Ge_x$ with Si and Ge P_b centers, electrons supplied by the P doping are preferentially captured by the Ge P_b centers and disactivate the centers. After the passivation of the Ge P_b centers is completed, the passivation of the Si P_b centers starts. This results in an improvement in the PL efficiency. Since the number of Ge P_b centers increases with increasing Ge concentration, a larger number of P atoms are necessary to completely passivate all of the P_b centers, i.e., to obtain the maximum PL efficiency. The present results demonstrate that P doping is an effective method for passivating the P_b centers and improving the PL efficiency of $Si_{1-x}Ge_x$ alloy nanocrystals. After the passivation of all P_b centers, further doped P atoms supply free electrons in nc-$Si_{1-x}Ge_x$. The free-electron absorption observation provides direct evidence that carriers in nanometer-sized $Si_{1-x}Ge_x$ alloy crystals can be supplied by impurity doping.

VI. ACKNOWLEDGMENTS

The authors are grateful to Kazutomi Shigeeda for his valuable assistance in this work. This work was supported by a Grant-in-Aid for Science Research from the Ministry of Education, Culture, Sports, Science and Technology, Japan, and a Grant for Research for the Future Program from the Japan Society for the Promotion of Science (JSPS-RFTF-98P-01203). K. T. would like to thank the Japan Society for the Promotion of Science for their financial support.

[1] H. Takagi, H. Ogawa, Y. Yamazaki, A. Ishizaki, and T. Nakagiri, Appl. Phys. Lett. **56**, 2379 (1990).
[2] S. Schuppler, S. L. Friedman, M. A. Marcus, D. L. Adler, Y.-H. Xie, F. M. Ross, Y. J. Chabal, T. D. Harris, L. E. Brus, W. L. Brown, E. E. Chanban, P. F. Szajowski, S. B. Christman, and P. H. Citrin, Phys. Rev. B **52**, 4910 (1995).
[3] Y. Kanzawa, T. Kageyama, S. Takeoka, M. Fujii, S. Hayashi, and K. Yamamoto, Solid State Commun. **102**, 533 (1997).
[4] M. Fujii, S. Hayashi, and K. Yamamoto, in *Recent Research Development in Applied Physics*, edited by S. G. Pandalai (Transworld Research Network, Trivandrum, 1998), Vol. 1, p. 193.
[5] S. Takeoka, M. Fujii, and S. Hayashi, Phys. Rev. B **62**, 16820 (2000).
[6] G. Polisski, H. Heckler, D. Kovalev, M. Schwartzkopff, and F. Koch, Appl. Phys. Lett. **73**, 1107 (1998).
[7] D. Kovalev, H. Heckler, M. Ben-Chorin, G. Polisski, M. Schwartzkopff, and F. Koch, Phys. Rev. Lett. **81**, 2803 (1998).
[8] G. Absreiter, *Light Emission in Silicon: From Physics to Devices* (Academic, New York, 1998), Vol. 49, p. 37.
[9] M. Fujii, D. Kovalev, J. Diener, F. Koch, S. Takeoka, and S. Hayashi, J. Appl. Phys. **88**, 5772 (2000).
[10] M. Schoisswohl, J. L. Cantin, M. Chamarro, and H. J. von Bardeleben, Phys. Rev. B **52**, 11898 (1995).
[11] S. Lebib, H. J. von Bardeleben, J. Cernogora, J. L. Fave, and J. Roussel, J. Lumin. **80**, 153 (1999).
[12] S. Takeoka, K. Toshikiyo, M. Fujii, S. Hayashi, and K. Yamamoto, Phys. Rev. B **61**, 15988 (2000).
[13] K. Toshikiyo, M. Tokunaga, S. Takeoka, M. Fujii, and S. Hayashi, J. Appl. Phys. **89**, 4917 (2001).
[14] S. P. Withrow, C. W. White, A. Meldrum, J. D. Budai, D. M. Hembree, Jr., and J. C. Barbour, J. Appl. Phys. **86**, 396 (1999).
[15] A. A. Seraphin, S.-T. Ngiam, and K. D. Kolenbrander, J. Appl. Phys. **80**, 6429 (1996).
[16] M. Fujii, A. Mimura, S. Hayashi, and K. Yamamoto, J. Appl. Phys. **75**, 184 (1999).
[17] M. Fujii, A. Mimura, S. Hayashi, K. Yamamoto, C. Urakawa, and H. Ohta, J. Appl. Phys. **87**, 1855 (2000).
[18] A. Mimura, M. Fujii, S. Hayashi, D. Kovalev, and F. Koch, Phys. Rev. B **62**, 12625 (2000).
[19] M. A. Renucci, J. B. Renucci, and M. Cardona, in *Light Scattering in Solids*, edited by M. Balkanski (Flammarion, Paris, 1971), p. 326.
[20] B. K. Meyer, D. M. Hofmann, W. Stadler, V. Petrova-Koch, and F. Koch, Appl. Phys. Lett. **63**, 2120 (1993).
[21] B. K. Meyer, D. M. Hofmann, W. Stadler, V. Petrova-Koch, F. Koch, P. Emanuelsson, and P. Omling, J. Lumin. **57**, 137 (1993).
[22] J. I. Pankove, *Optical Process in Semiconductors* (Dover, New York, 1971), p. 74.
[23] M. Lannoo, C. Delerue, and G. Allan, J. Lumin. **70**, 170 (1996).
[24] V. Petrova-Koch, T. Muschik, G. Polisski, and D. Kovalev, Mater. Res. Soc. Symp. Proc. **358**, 483 (1995).